Cepite, Daiga; Jakovics, Andris; Halbedel, Bernd; Krieger, Uwe:

Modelling of EM glass convection

URN: urn:nbn:de:gbv:ilm1-2014210117

Published OpenAccess: September 2014

Original published in:

Compel : international journal of computation & mathematics in electrical & electronic engineering. - Bradford : Emerald (ISSN-p 0332-1649). - 27 (2008) 2, S. 387-398.

DOI: 10.1108/03321640810847670

URL: http://dx.doi.org/10.1108/03321640810847670

[Visited: 2014-09-02]

COMPEL - The international journal for computation and ma... in electrical and electronic engineering

Modelling of EM glass convection

D. Cep#te A. Jakovi#s B. Halbedel U. Krieger

Modelling of EM glass convection

D. Cepīte and A. Jakovičs
Laboratory for Mathematical Modelling of Environmental and Technological Processes University of Latvia, Riga, Latvia, and

B. Halbedel and U. Krieger
Glass and Ceramic Technology Group, Faculty of Mechanical Engineering, Inter-faculty Institute of Materials Science, Technical University Ilmenau, Ilmenau, Germany

Abstract

Purpose – To develop the mathematical model, which allows predicting the temperature and flow distribution of an opaque glass melt with the temperature-dependent properties in case it is generated by electromagnetic and thermal convection. Analysis has been done for geometry of the model crucible with the immersed rod electrodes. Numerical analysis is used as a tool for finding out the parameters of the system, which allow getting desiderated homogeneity of temperature field by EM action.

Design/methodology/approach – ANSYS CFX software is implemented for coupling of EM, thermal and HD processes in the modelled system. Usability of non-inductive approximation is shown using a full harmonic analysis in ANSYS.

Findings – External magnetic field can impact the temperature distribution in the whole volume of the melt significantly, it relocates the hottest zones and changes the maximal temperature in the melt. Qualitative agreement between the numerical and experimental results has been obtained. Dependence of the potential difference between the electrodes on the velocity and temperature range has been examined. Impact of different thermal boundary conditions has been analysed.

Research limitations/implications – Effects analysed in the publication occur in each conducting media subjected to the impact of simultaneous electrical and magnetical field. The main limitation is non-transparency of the melt.

Practical implications – The purpose is to develop a mathematical tool for parameter optimisation of real glass melting furnace.

Originality/value – In the present model temperature dependent properties of the melt have been taken into account, which has been neglected in previous models.

Keywords Mathematical modelling, Glass, Furnaces, Temperature, Electromagnetism

Paper type Research paper

Introduction

The experiments carried out in the laboratory system reported in Huelsenberg *et al.* (2004) have shown that an external magnetic field plays an important role in homogenisation of temperature field as well as in the chemical homogeneity of the glass melt in special melting furnace (Figure 1). Experimentally measured vertical temperature profiles are used to characterise the impact of Joule heat sources and an external electromagnetic (EM) field on temperature homogeneity of the melt. The temperature range of the vertical temperature profiles has decreased in case the external magnetic field has been imposed on the system. One dimensional model (the glass motion inside the crucible has been replaced with the analysis of the flow inside the circular loop) and analysis of interaction between thermal and EM convection taking place in the experiment has been reported in Giessler *et al.* (2005); the

COMPEL: The International Journal for Computation and Mathematics in Electrical and Electronic Engineering
Vol. 27 No. 2, 2008
pp. 387-398

0332-1649
DOI 10.1108/03321640810847670

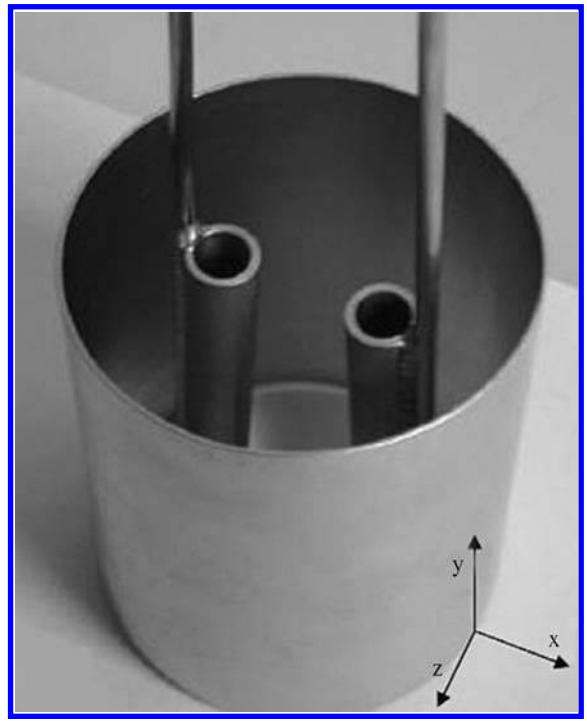

Figure 1.
Image of the platinum crucible with the rod electrodes

results allow estimating the influence of characteristic parameters of the system on stability of the process. The mathematical model presented here is developed to show the character of the flow and temperature distribution in a complete 3D volume of the melt. Solution for coupled EM, hydrodynamics and heat transfer processes in the region of the cylindrical volume of the melt with immersed hollow rod platinum electrodes is obtained.

Experimental set-up

Basically the experimental set-up which is described in detail in Huelsenberg *et al.* (2004) consists of a cylindrical platinum crucible (inner diameter 8 cm) with two symmetrically immersed platinum electrodes.

The level of the melt is 8 cm and the electrodes are immersed 6 cm deep. AC with a frequency of 50 Hz is flowing in the melt between the electrodes which results in a Joule heat production. The crucible is inserted in an isolated furnace which is placed in the air gap between the EM poles. Alternating magnetic field with the magnetic induction **B** oriented in z direction is imposed on the system in order to generate the Lorentz force distribution which intensifies the stirring process (Figure 1). The effective value of the external magnetic field is $B = 0.044$ T. Direction of the Lorentz force depends on a phase shift α_{ph} between **j** and **B**. In the case of $\alpha_{ph} = 0°$ the Lorentz force is upward-oriented in the region between the electrodes and it is acting in the same direction as a thermal convection and intensifying the flow.

Mathematical model

Particularity of EM problem

Since, the crucible with the melt have been inserted in an alternating magnetic field and the electrical current is flowing between the electrodes, then in general the inductive effects are able to impact the distribution of the averaged Lorentz force density $\mathbf{F} = Re\{\mathbf{j} \times \mathbf{B}^*\}$ (effective values have been used) – an alternating current which flows between the electrodes generates an alternating magnetic field. At the same time – an alternating external magnetic field is able to change a current distribution in the melt. In a particular experimental system the frequency of the electric and magnetic field is 50 Hz, electrical conductivity of the melt does not exceed 10 S/m, respectively, the induction effects do not play significant role in EM part of the problem and can be neglected. This is the first assumption of the model. Detailed EM analysis has been done to ascertain that it is reasonable. Results on this issue are presented in Cepīte *et al.* (2007). Lorentz force distribution is generated due to interaction between two independent physical fields **j** and **B**. Distribution of the electrical current in the melt is obtained by solving the continuity equation for the electric current:

$$\mathrm{div}(\sigma(T)\mathrm{grad}\varphi) = 0 \tag{1}$$

The second assumption of the model has been made concerning the BC for the electric potential: potential distribution in the electrodes has been assumed to be equipotent due to the high ratio of the electrical conductivities of platinum and the melt ($\sigma_{\mathrm{Platinum}}/\sigma_{\mathrm{melt}} \approx 10^5$).

Hydrodynamics of the melt

The motion of the melt is governed by the balance of the Lorentz force, thermal convection and viscous friction forces. The flow of the melt is laminar with the typical Reynolds number ≈ 1. Lorentz force and buoyancy force ($\mathbf{f}_c = \beta(T - T_0)g$, where $\beta = -\rho^{-1}(\partial\rho/\partial T)_p$) calculated in the Boussinesque approximation are included as the additional forces in a Navier Stokes equation determining the flow. No slip BC for the velocity of the melt has been used on the surface of the electrodes and on the crucible wall.

Thermal problem

In the experiments opaque glass melt has been used. Transparency measurements show that 1 mm of the melt absorbs ≈ 65 per cent of the radiation of the corresponding wavelength. Consequently, the radiation heat exchange inside the volume of the melt can be neglected. It is assumed that the radiation heat flux $q = \varepsilon\sigma_{StB}(T^4 - T_{\mathrm{ref}}^4)$ is leaving the free surface of the melt ($\varepsilon = 0.6$ has been used). In general, more complicated heat reflection might exist in the closed gaseous region above the free surface of the melt, which is not included in the mathematical model. Inside the melt conductive and convective heat transfer takes place. Joule heat production $s = \mathbf{j}^2/\sigma$ (in the melt) is included as a source term for the energy equation. The fixed temperature BC $T = T_{\mathrm{d}}$ has been applied on the crucible wall. It has been chosen by assuming that platinum conducts the heat well enough to equalize the temperature distribution on the internal surface of the crucible. As we have shown further in the text that might not be always true. That is the reason why the thermal BC has been varied and its general form (a heat flux BC) has been implemented.

Heat flux leaving the side and bottom wall of the melt has been set to $q = \alpha(T - T_s)$, where α is a heat transfer coefficient of a convective heat transfer and T_s – temperature of surroundings. In case $\alpha \rightarrow \infty$ $T \rightarrow T_s$ – what means the same as the fixed temperature BC.

Experimentally found temperature dependencies of the electrical conductivity σ, thermal conductivity λ, dynamic viscosity η, density ρ used in our calculations are mathematically presented as:

$$\rho(T) = A_\rho \cdot T + B_\rho$$

$$\sigma(T) = A_\sigma \cdot \exp\left[-\frac{B_\sigma}{T}\right]$$

$$\lambda(T) = A_\lambda \cdot T^2 + B_\lambda \cdot T + C_\lambda$$

$$\eta(T) = A_\eta \cdot \exp\left[\frac{-1}{(B_\eta \cdot T^2 + C_\eta \cdot T + D_\eta)}\right]$$

where A_i, B_i, C_i, D_i are approximation constants.

The nature of the intensification of the coupling between EM, thermal and HD processes due to the temperature-dependent properties of the melt can be illustrated in a following way: the distribution of $\mathbf{F}$ depends on temperature due to $\sigma = \sigma(T)$. $\mathbf{F}$ modifies the distribution of the temperature as well as the distribution of the temperature is changed by the Joule heat production s and buoyancy. Consequently, the distribution of $\mathbf{F}$ is modified.

Both – steady state and transient solution methods have been implemented in solving the mathematical problem.

Implementation

Ansys software is used for solving the mathematical problem. Simulation domain consists of the fluid with two solid inclusions (electrodes). Top view of the geometry of the system and the BC are shown in Figure 2. Mesh used for the numerical modelling of the coupled problem consists of $\approx 1.5 \times 10^5$ elements (Figure 3(a)). One fourth part of the system has been used in a solution process. Asymmetric modes of the flow have been assumed to be negligible. It is reasonable for a laminar flow what is exactly the case of the particular system. The only instabilities which might occur in the melt are connected with significantly temperature-dependent properties of the melt. All imbalances below 1 per cent and the maximal residual below 10^{-5} are used as the target criteria for the convergence of the solution. Platinum crucible and surroundings are not included in the numerical discretisation of the coupled problem. Instead of that a full harmonic EM analysis (mesh shown in Figure 3(b)) has been done to determine and verify the BC of the reduced system. The results of the full harmonic EM analysis show that the potential drop on the electrode surface is less than 0.2 per cent; this result ascertains that the choice of the BC for the potential is reasonable. The changes in magnetic field distribution due to the induced magnetic field around the electrodes (Figure 4(a)) are expected to be below 2 per cent of the magnitude of the external magnetic field.

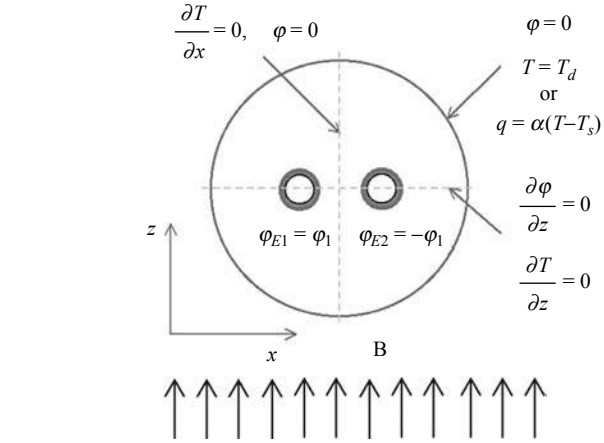

Figure 2.
Sketch of the model: volume of the melt with the two immersed hollow platinum electrodes (top view) and its boundary conditions

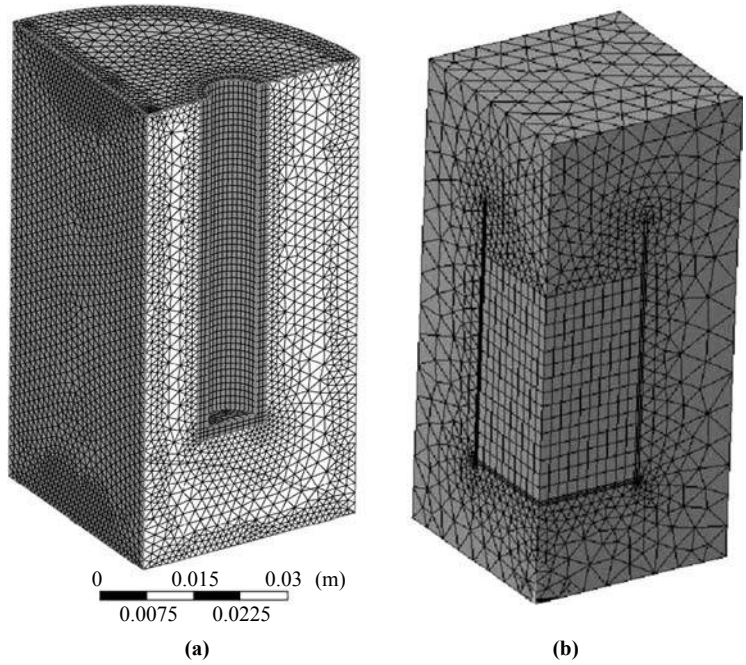

Figure 3.
The mesh used for coupled HD: (a) EM and thermal calculation; (b) the mesh used for harmonic EM analysis

In Figure 4(b) the distribution of the electric current induced in the crucible wall (2 mm in thickness) has been illustrated. The electric current revolves around the direction of the external magnetic field. The magnitude of the current which is induced inside the melt (electrical conductivity of the melt is assumed to be 8 S/m) is less than 0.1 per cent of the magnitude of the maximal current flowing between the electrodes. Consequently, the induction effects are not included in a coupled problem what facilitate the solution process significantly. In this situation data exchange between Ansys Classics and Ansys Cfx in each time step is not necessary. An alternative way of coupling between

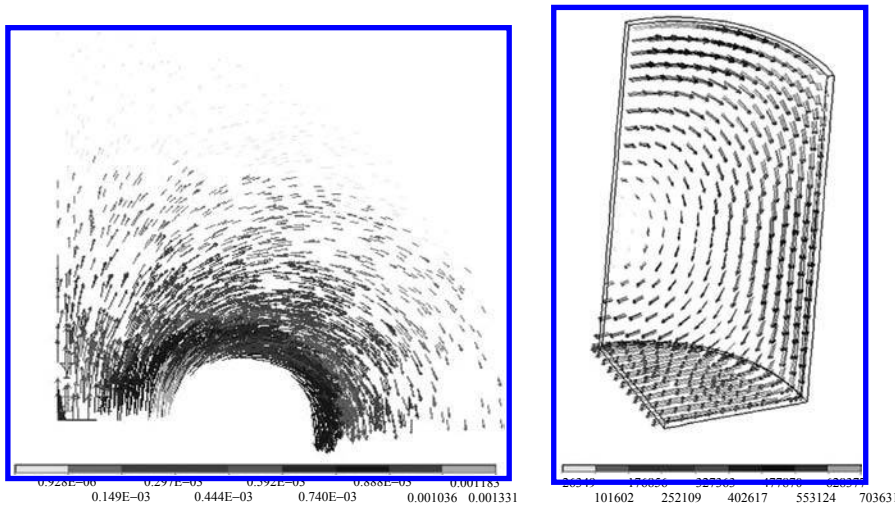

Figure 4.
(a) Magnetic field around the electrode in case $U_{\text{eff}} = 27$ V and $f = 50$ Hz; (b) induced current in A/m^2 in the platinum crucible due to the external homogeneous alternating magnetic field ($f = 50$ Hz)

the processes (using only the environment of Ansys Cfx) has been realised. Hydrodynamics and heat transfer problems are implemented in Ansys Cfx automatically, but EM has been added by adapting transport equation to the particular requirements of the mathematical model. The transport equation has been modified to permit calculation of the continuity equation (1) for the electric current. The fixed value of the electric potential $\varphi = 0$ has been set on the contact surface of the melt and the crucible. The effective potential $\varphi_1 = \pm U_{\text{eff}}/2$ has been chosen on the electrode contact surface with a melt. Consequently, the distribution of the electric potential is obtained. It allows calculating the electric current density $\mathbf{j} = -\sigma(T)\text{grad}\varphi$ that is necessary for computing the Joule heat production rate and the distribution of the Lorentz force.

Results

Basic interrelations

Joule heat production rate is one of the characteristic parameters of the experiment. Figure 5(a) shows dependence of integral Joule heat production rate and the maximal velocity on parameter T_{ref}. Joule heat production rate is higher in case $B = 0$; the melt flow is slower – it takes longer time for the melt element to flow along the hottest zone in the region between the electrodes. It results in heating up and larger Joule heat production rates. General dependence of integral Joule heat production rate and the maximal velocity on parameter U_{eff} predicted by our model is shown in Figure 5(b). Joule heat production rate shows steep, almost linear increase in case U_{eff} goes up. For a fixed value of U_{eff} the velocity is at least three-fold larger in case the external magnetic field is imposed on the system. It is observable that the difference between Joule heat production rates decreases in case U_{eff} is lowered. In case $U_{\text{eff}} \approx 21$ V there is almost no impact of the external magnetic field on the Joule heat production rate (Figure 5(b)); for larger values of U_{eff} the input parameter of the model U_{eff} should be

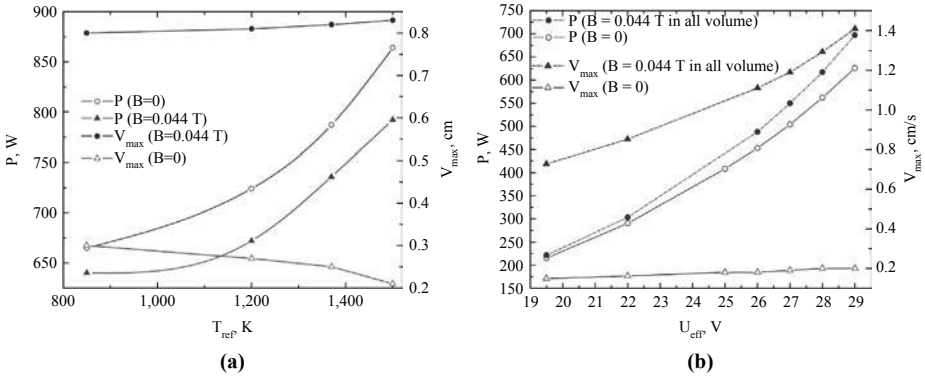

Figure 5.
Joule heat production rate and the maximal velocity v_{max}: (a) for different values of T_{ref}; (b) for different values of U_{eff}

Note: In case (a) the magnetic field is imposed only in the region between the electrodes

increased approximately by 0.5 V (in case $B = 0$) to reach the same Joule heat production rate as it is in case $B = 0.044$ T. In the parameter range we have analysed – stationary solution can be found by both – steady state and transient solution methods. Nevertheless, for higher maximal temperatures a non-stable solution might be possible.

Figure 6 shows typical numerical axial temperature profiles in case $B = 0$ and $B = 0.044\,\mathrm{T}(\alpha_{ph} = 0°)$. According to numerical results the character of the profile is typical for the arrangement of the external magnetic field and it does not change strongly in case the parameter U_{eff} is varied. On the contrary, large horizontal temperature gradient in the central part of the melt is the reason why the temperature profiles on the two vertical axis, which are located only 3 mm distant each of other (both scattered circles shown in Figure 6(b)), differ very much. It is worth mentioning that the experimental results lie in-between the numerical results. The numerical results as well as the experiment ascertain that magnetic field ($\alpha_{ph} = 0°$) is able to diminish the temperature range on the axis of the system. Nevertheless, disadvantages of the model remain experiments show that:

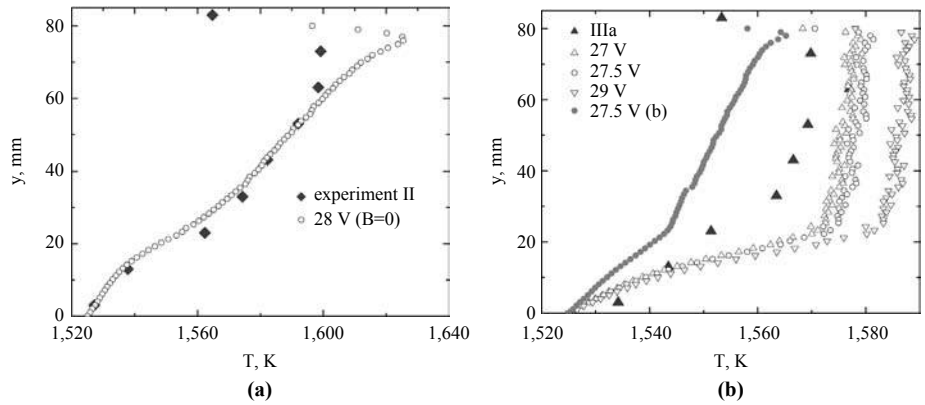

Figure 6.
Experimentally (II and IIIa with $P = 575$ W) and numerically gained ($T_d = 1{,}525$ K, $T_{ref} = 1{,}500$ K) axial temperature profiles for different values of parameter U_{eff}: (a) $B = 0$; (b) $B = 0.044$ T

- temperature in the vicinity of the crucible bottom is observably different for cases $B = 0$ and $B \neq 0$ (Figure 6);
- it is a function of the total power input; and
- temperature in the vicinity of the crucible bottom is not spatially uniform (two axis on which the experimental measurements have been done are shown in Figure 9).

Till now the first point has been neglected in our model, the second point has been solved by adapting T_d according to temperature profiles for the total power inputs 575 and 700 W which are known from the experiment. The third point has turned out to be the most important reason to modify the model.

Analysis of the impact of thermal BC on temperature distribution

On the one hand, the heat flux BC is preferable in comparison with the fixed temperature T_d set on the boundary because it allow different temperatures in different locations on the crucible bottom, on the other hand it make analysis more complicated because in general α might be a function of the flow near the border and may vary along the surface of the crucible wall. At this analysis such possibility is assumed to be negligible.

Figure 7 is used to illustrate the difference between the temperature profiles gained with a fixed temperature and heat flux BC. In selection of parameter T_s it has been assumed that it should not be greater than minimal temperature (known experimentally) in the vicinity of the crucible bottom in case the melt flow is weak ($B = 0$). Although the temperature difference on the crucible bottom according to the measurements on the two vertical axis does not exceed 10°K the temperature difference on a whole crucible wall (according to numerical calculations) can exceed 50°K or more due to the chosen heat flux BC (Figure 8).

Experiments show that temperature in the vicinity of the bottom wall is lower on the peripheral axis than on the central axis (Figure 7). That is true for all arrangements of the external magnetic field examined experimentally. The value of the difference and the temperature range is impacted by both – the magnitude of the Joule heat production rate and the arrangement of the external magnetic field. Figure 7 shows that a heat flux BC ensures qualitatively the trend in changes of temperature in the vicinity of crucible bottom and the trend is consistent with the experiment.

Impact of the external magnetic field on the temperature distribution in the melt according to numerical results in case the fixed temperature T_d is set on the side and bottom walls of the crucible is presented in Cepīte *et al.* (2007). Figure 9 shows the temperature and velocity distribution in a whole volume of the melt in case the heat flux BC has been applied. Qualitatively the force on temperature distribution acts similarly as in case the fixed temperature BC T_d is used: in case of B $\neq 0$ ($\alpha_{ph} = 0°$) the hottest zone is moved outside the centre of the crucible and it is located deeper than in case of $B = 0$. In case $B = 0$ the flow in xy plane is not predominant and slow upward-oriented motion on the opposite side of the electrode is observable. It is worth mentioning that a total temperature difference has decreased in case the external magnetic field is applied what is in agreement with the experiment. In contrast, the temperature and velocity distribution in the melt in case $B = 0.044$ T and $\alpha_{ph} = 180°$ is shown in Figure 10. The Lorentz force diminishes the velocity in the central part of the

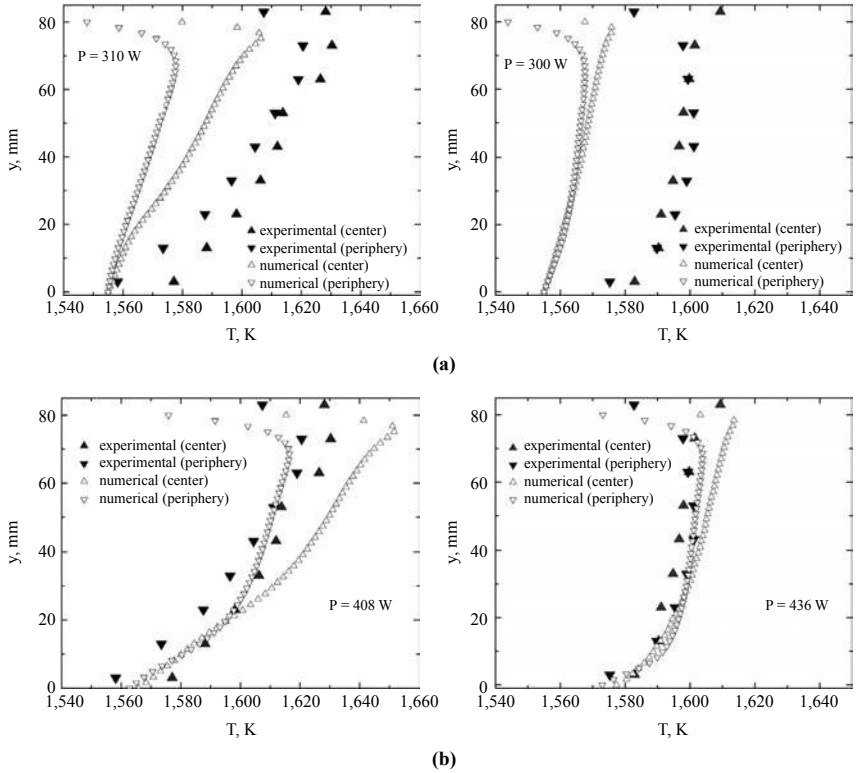

Figure 7.
Vertical temperature profiles – experimental and numerical ($U_{eff} = 20$ V, $T_{ref} = 1{,}500$ K) results. Thermal boundary conditions on the crucible wall: (a) fixed temperature $T_d = 1{,}555$; (b) $\alpha = 180$ W/Km^2, $T_s = 1{,}545$ K

Notes: Experiment: Joule heat production rate $P = 700$W, for numerical results P values are written inside each chart. Left: $B = 0$T, right: $B = 0.44$T

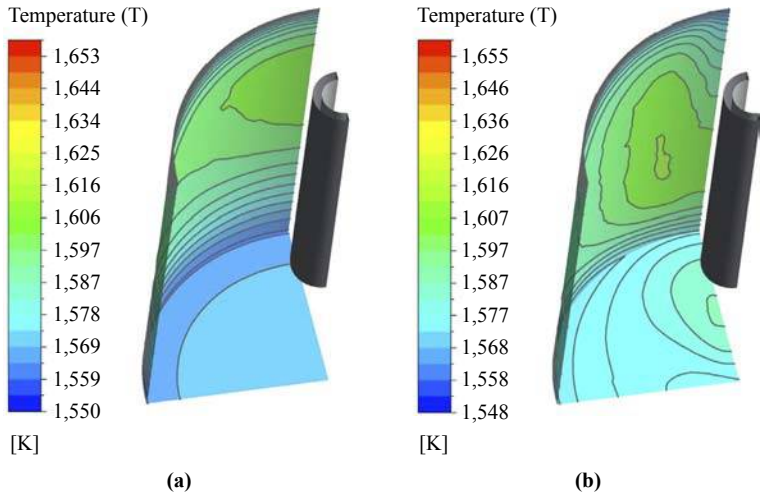

Figure 8.
An example of the temperature distribution (numerical results with $\alpha = 180$ W/Km^2, $T_s = 1{,}545$ K) on a crucible wall: (a) $B = 0$ T; (b) $B = 0.044$ T

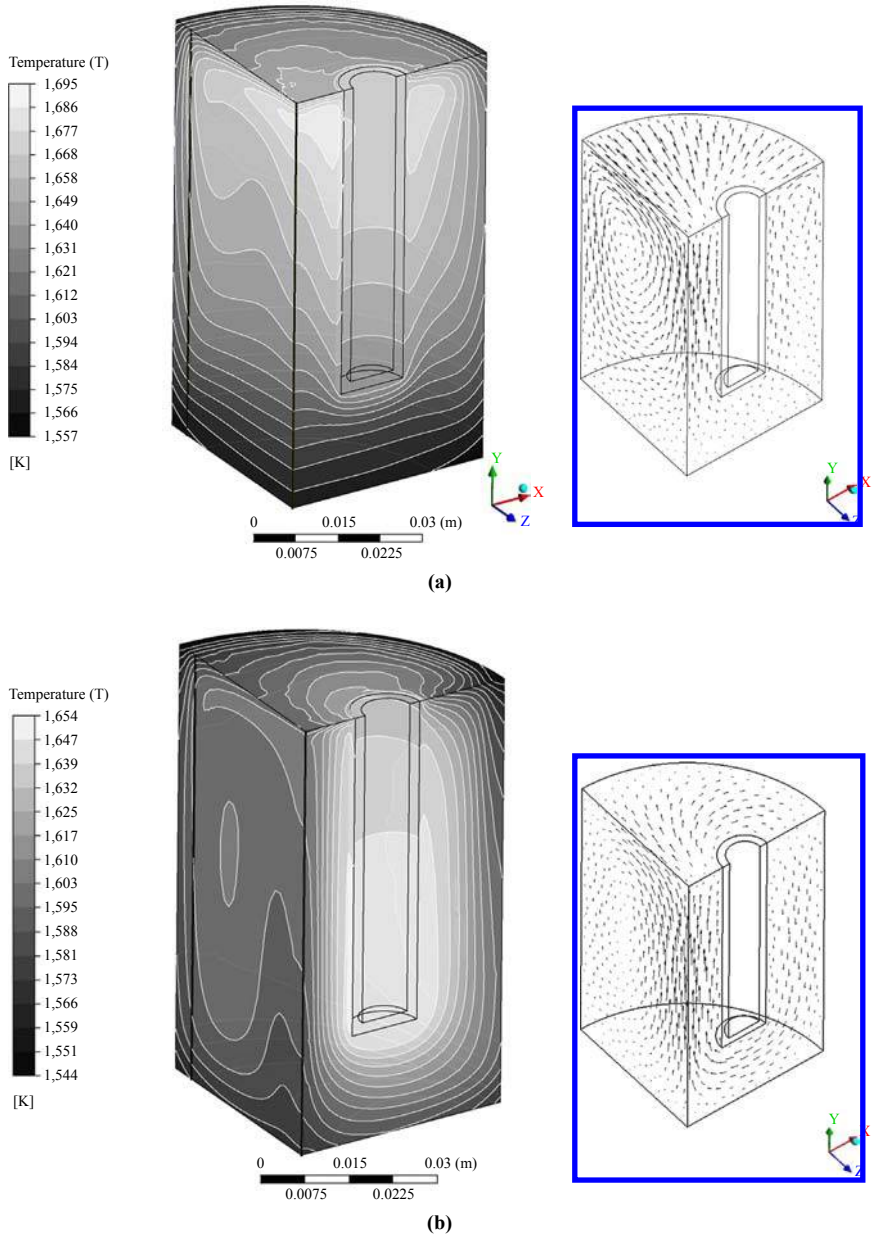

Figure 9.
An example of temperature and velocity distribution (numerical results): (a) $B = 0\,\mathrm{T}$; (b) $B = 0.044\,\mathrm{T}$, $\alpha_{ph} = 0°$

Note: Vertical axes on which the experimental temperature measurements take place are highlighted in the left column (temperature profiles in fig.7). Maximal velocity (a) 0.2 cm/s; (b) 1.6 cm/s

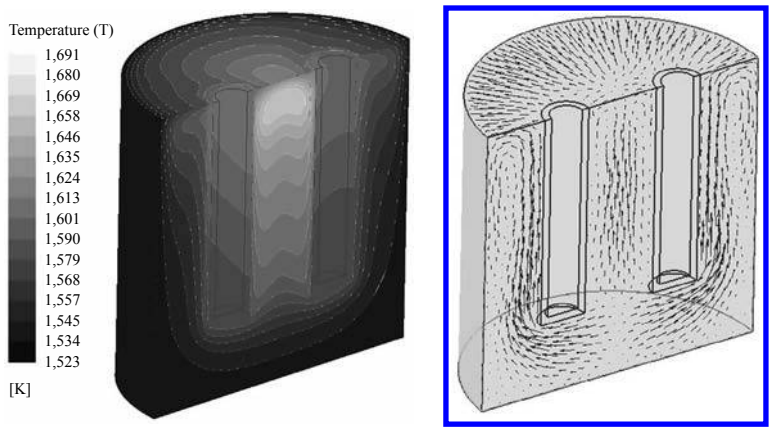

Note: Maximal velocity 0.2 cm/s

Figure 10.
(a) Temperature distribution in the system; (b) velocity distribution in the system in case of $\alpha_{ph} = 180°$ ($T_d = 1{,}525$ K)

melt and the hottest zone is not able to leave the central region similarly as in case $B = 0$.

For a fixed value of U_{eff} a Joule heat production rate predicted numerically is lower than observed in the experiment. Since, the non-inductive approach and BC for the EM problem are proved as valid, the reasons for that are connected with a choice of the thermal BC of the model.

Conclusions

Previous illustrations show that the model is able to give a good qualitative estimation of the processes taking place in the system for the cases $B = 0$ and $B \neq 0$. It has been illustrated that there exist the potential values for which the Joule heat production rate is weakly impacted by the applied external magnetic field despite the fact that a difference between the maximal velocities is significant. According to the numerical model homogeneous external alternating magnetic field can be used to relocate the hottest zones in the crucible: in case $B = 0$ the maximal temperature is located in the upper central part of the crucible; in case $B \neq 0$, $\alpha_{ph} = 0°$ it is relocated to the opposite side of the electrode near its bottom; in case $B \neq 0$, $\alpha_{ph} = 180°$ the hottest region is in the central part (similarly as it is without the magnetic field) only due to suppression of thermal convection the level of temperature is higher.

It has been shown that the non-inductive approximation in a particular range of parameters is reasonable (taking into account the inductive effects for calculations in glass melts was noted as an open question in Giessler *et al.* (2005)). The main shortage of the model is the offset between the experimentally and numerically observed Joule heat production rates for a given U_{eff}. One of the reasons might be the dependence of the parameters T_s and α in the heat flux BC on the flow velocity. Radiation heat exchange inside the interior of the melt is going to be included in the model in the future; it would allow verification of the numerical results with the experimental data obtained for the transparent glass melts.

References

Cepīte, D., Jakovičs, A., Halbedel, B. and Krieger, U. (2007), "Modelling of the 3D glass melt flow driven by EM and thermal convection", *Proceedings of the Fifth Baltic Heat Transfer Conference, St Petersburg*, pp. 112-21.

Giessler, C., Sievert, C., Krieger, U., Halbedel, B., Huelsenberg, D., Luedtke, U. and Thess, A. (2005), "A model for electromagnetic control of buoyancy driven convection in glass melts", *Fluid Dynamics & Materials Processing*, Vol. 1 No. 3, pp. 247-66.

Huelsenberg, D., Halbedel, B., Conrad, G., Thess, A., Kolesnikov, Y. and Luedtke, U. (2004), "Electromagnetic stirring of glass melts using Lorentz forces – experimental results", *Glass Science and Technology*, Vol. 77 No. 4, pp. 186-93.

Corresponding author

D. Cepīte can be contacted at: daiga.cepite@lu.lv